Nano-mapping Material Interfaces via Hot Electrons

K. E. J. Goh* and C. Troadec

Institute of Materials Research and Engineering, Agency for Science, Technology and Research (A*STAR), 3 Research Link,Singapore 117 602, Singapore,
* kejgoh@yahoo.com

ABSTRACT

As devices shrink below 100 nm in size, nanoscale imperfections (due to defects and contaminants) at material interfaces become significant perturbations to ideal device characteristics and in some cases can dominate the device behavior. Of increasing importance therefore is the ability to measure local variations in the critical material interface of a device with nanometer resolution and correlate them to the overall device behavior. Toward this end, we have developed a dual-parameter technique to map Schottky-like interfaces with nanometer lateral resolution based on hot electron spectroscopy. Here, we present results of this method of analysis on the well-known Au/Si interface, highlighting the particular sensitivity for detecting changes in device behavior due to nanoscale contaminations like organic molecules and carbon nanotubes. Such analyses are expected to provide crucial insights into how the combination of materials and the use of different processing conditions affect the performance of nanodevices.

Keywords: interface, hot electrons, ballistic electron emission microscopy/spectroscopy (BEEM/BEES), barrier height, transmission

1 INTRODUCTION

According to the 2010 International Technology Roadmap for Semiconductors [1], production at the 24 nm node is expected to begin sometime in 2011. The relentless scaling of semiconductor devices has now reached a level where the critical device dimensions are no more than a few tens of nm, and this includes gate dielectric layers which can be less than 1 nm (i.e. a few atomic layers thick). Defects (interface traps, impurities, grain boundaries, interstitials) of the size on the order of 1 nm can now significantly alter the functions of devices, and the device yield for a manufacturing process depends more than ever on the ability to control the quality of material interfaces at the nm level. While the structural and compositional properties may be elucidated by HRTEM (High Resolution Transmission Electron Microscopy) and EELS (Electron Energy Loss Spectroscopy), a non-invasive assessment of the local charge transport properties at such interfaces covering areas of ~100 nm^2 can be very challenging and does not currently exist for the manufacturing line. To date, the only technique capable of non-invasive assessment of a buried interface with nm resolution relies on the use of hot electrons to probe the interface in what is known as Ballistic Electron Emission Microscopy/Spectroscopy (BEEM/BEES) invented by Bell and Kaiser in 1988 [2, 3]. This technique has since been used to study a variety of material interfaces typically buried under a few nm of metal, including metal/semiconductor [2, 3, 4, 5, 6], metal/oxide/semiconductor [7, 8, 9, 10], metal/organic/semiconductor [11, 12], and more exotic ones involving multilayer-heterostructures [13, 14]. A key advantage is that BEEM is based on Scanning Tunneling Microscopy (STM) which offers high spatial resolution.

In this paper, we demonstrate that nm-scale information extracted from local BEES measurements for the well-known Au/Si interface is sensitive to “contamination” layers (organic molecules, and carbon nanotubes) of only few atoms to few nm thick inserted at the interfaces. We propose a dual-parameter representation (based on the interface barrier height and transmission) as a possible way to classify and map such material interfaces based on local charge transport information, and discuss the potential of this representation for analysing nanoscale devices.

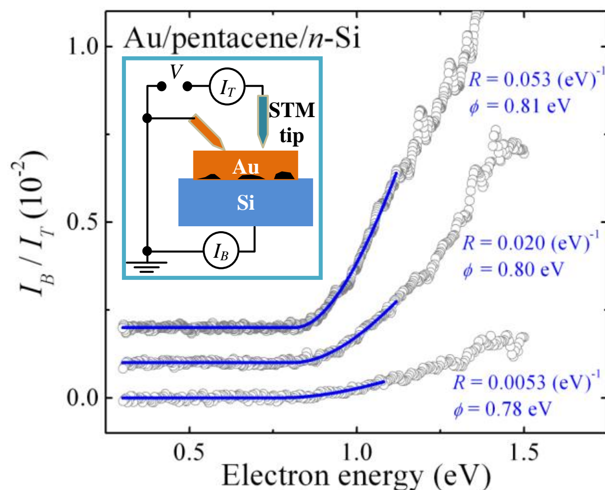

Figure 1: BEES spectra showing different electron transmissions and the associated electronic barrier at three different locations on a sample with a nominal coverage of approximately a monolayer of pentacene sandwiched between the top Au electrode and the n-Si(111) substrate. Solid blue lines are fits to the Bell-Kaiser model. Inset: A schematic of the typical setup for BEEM/BEES.

NSTI-Nanotech 2011, www.nsti.org, ISBN 978-1-4398-7142-3 Vol. 1, 2011

2 HOT ELECTRON SPECTROSCOPY

Hot electrons (or holes) injected directly into a metal/semiconductor interface from the metal side can be used to probe the transport properties at the interface. If the metal layer is kept sufficiently thin so that the electrons (or holes) propagate without energy loss (ballistically), then they arrive at the interface with a well-defined energy which allows the quantitative assessment of properties such as the local interface barrier height ϕ. This is the basic principle of operation for BEEM.

2.1 Three-terminal STM Setup

The typical setup of a BEEM measurement is shown in the inset of Fig. 1. It is essentially a 3-terminal extension to the standard 2-terminal STM measurement, where the additional terminal is the collector for the BEEM current I_B (arising from electrons that cross the interface) formed by an ohmic contact at the back of the substrate. The metal overlayer that buries the interface is commonly called the base and forms the grounding for conventional STM. In BEEM imaging mode, the STM tip is typically kept at a fixed bias V just above the barrier height of, say, a metal/semiconductor interface under study. This provides a qualitative assessment of interface homogeneity based on a spatial map of the BEEM current collected. In spectroscopy mode (i.e. BEES), the STM tip is held over a particular spot on the sample and the tip bias V is ramped over the energy range of interest while maintaining a constant tunneling current I_T. In Fig. 1, we show 3 BEES spectra obtained from a sample where an inhomogenous layer of pentacene molecules has been sandwiched between Au and an *n*-Si(111) substrate [11]. From such spectra, one may extract useful information on the interface barrier and transmission using the Bell-Kaiser model which is discussed next.

2.2 Bell-Kaiser Model

The Bell-Kaiser (BK) model is most often used for analysing BEES spectra. It includes various simplifying assumptions such as planar tunneling formalism, energy-independent attenuation of the tunneling current due to scattering processes, and conservation of electron energy and transverse momentum at the metal/semiconductor interface. Nevertheless, this simple model can often adequately describe the dominant behaviour in experimental BEES spectra, especially for the energies just above the threshold energy of the interface barrier. Details of the BK theory are found in the original paper [3] and are also described in a number of reviews on BEEM which include some extensions of the theory [15-18]. Here, we shall only provide the key equation relevant to the dual-parameter analysis proposed in Section 2.3. In practical use, the BK model simplifies for closed-loop BEES [15] to a power law in electron energy (eV) given by

$$\frac{I_B}{I_T} = R\frac{(eV-\phi)^n}{eV} \tag{1}$$

where ϕ is the local interface barrier, R is the transmission attenuation, and n is 2 for the simple BK model [3, 15] which assumes free electron behaviour and energy independent transmission, although Prietsch [19] has suggested $n = 5/2$ is more appropriate for situations where transmission is energy dependent (e.g. due to electron-electron scattering, quantum mechanical reflection, etc.). Most reports find $n = 2$ describes experimental data well, and using $n = 5/2$ often produces a small systematic correction in ϕ that is only of the order of $(3/2)kT$ [15, 16]. In the following analysis, we use only $n = 2$ for data fitting in order to provide a consistent treatment of the BEES spectra for the purpose of comparison.

2.3 Dual-parameter Analysis of BEES Data

The use of Equation (1) for fitting BEES spectra results in the extraction of the parameters R and ϕ as illustrated in Fig. 1. A systematic map of these parameters over an interface of interest can reveal in a non-invasive way nanoscale artifacts in the buried interface [12]. In addition, the careful sampling of these parameters [20] allows the extraction of useful device parameters [21] such as the interface trap density and charge neutrality level. In Section 3, we shall demonstrate that a 2-dimensional density plot of R and ϕ could be useful for identifying and understanding modifications to the well-known Au/Si interface.

3 EXPERIMENTAL

BEES measurements were performed in a home-built BEEM system described elsewhere [12]. BEES measurements were performed under closed-loop control for the STM tip. The BEES spectra were fitted to Equation (1) with $n = 2$ within 0.3 – 0.5 eV of the threshold voltage where I_B starts to increase. For the dual-parameter analysis, more than 500 to a few thousand spectra were typically taken over different regions on each device in order to ensure statistical validity.

We consider 4 samples here in order to compare how the R-ϕ density plots are modified as a result of modifications to the Au/Si interface:

Sample 1: Au/*n*-Si
Sample 2: Au/pentacene (1.5nm)/n-Si
Sample 3: Au/Triton-X100/n-Si
Sample 4: Au/SWNT+Triton-X100/n-Si.

All samples were 6×6 mm^2 *n*-type Si(111) wafers (1 – 10 Ω cm) which had been As-implanted on the backside to form ohmic back-contacts. The detailed preparations of

BEEM compatible diodes on Samples 1 and 2 had been reported elsewhere [12]. Essentially, Sample 1 serves as the control Au/*n*-Si sample. For Sample 2, we inserted nominally a monolayer of pentacene (~1.5 nm) via sublimation before depositing the Au electrode. For Samples 3 and 4, we used a solution of ~2% (v/v) Triton-X100/DI(De-Ionized) water and sample preparation was carried out in a nitrogen environment. Only the Triton-X100 surfactant was introduced onto Sample 3 via drop-casting. For Sample 4, single-walled carbon nanotubes (SWNTs) were first dispersed in the Triton-X100/DI solution and sonicated for several minutes before being drop-casted onto the substrate, left to settle for 30 min and dried by nitrogen. This resulted in a sparse distribution of about 1 SWNT per 1 μm^2. (Note that Triton-X100 was used to promote adhesion of the SWNTs to the Si surface.) Care was taken to keep the solution only on the top of the substrate for both Samples 3 and 4. Au electrodes (~15 nm thick) were evaporated on following a brief etch in 7% HF.

4 RESULTS & DISCUSSION

Figure 2 shows the representative R-ϕ density plot for the simple Au/n-Si interface. The data points essentially gravitate to the binome (0.82 eV, 0.05 $(eV)^{-1}$). The spread in ϕ is attributed to the typical inhomogeneity of a heterojunction Schottky interface while the spread in R reflects variations in both the Au layer and the interface.

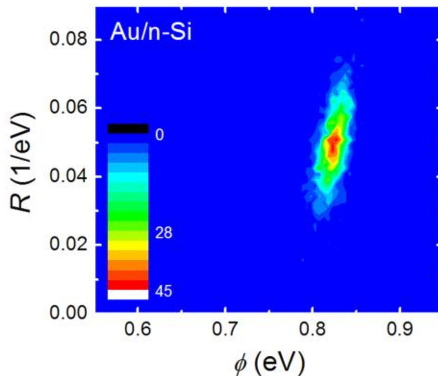

Figure 2: R-ϕ density plot for a Au/n-Si(111) interface (Sample 1).

If we now insert a monolayer of pentacene molecules into this Au/n-Si interface, the R-ϕ density plot morphs into the spur-like distribution shown in Fig. 3. This distribution shows a main peak around (0.76 eV, 0.002 $(eV)^{-1}$) with a long tail leading towards the Au/n-Si binome in Fig. 2. This has been attributed to the rather inhomogeneous pentacene layer and a detailed analysis of this distribution may be found in References 12, 20 and 21. The key point to note here is the pronouncedly different R-ϕ distribution compared to Fig. 2.

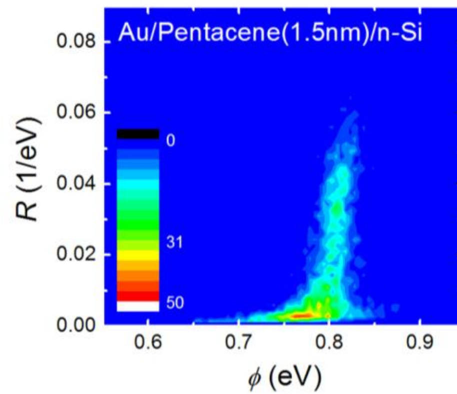

Figure 3: R-ϕ density plot for a Au/Pentacene/n-Si(111) interface (Sample 2).

Changing the "contamination" layer to Triton-X100 (which is really a control for the next sample), we again see a significantly different R-ϕ distribution in Fig. 4. This new distribution has a dominant peak around the binome (0.75 eV, 0.01 $(eV)^{-1}$). While the Triton-X100 layer appears to have a smaller spread in R, the inhomogeneity introduced in ϕ is about the same as that caused by the pentacene layer. The transmission associated with the peak of the distribution also appears to be higher by a factor of ~5 compared to that for Sample 2.

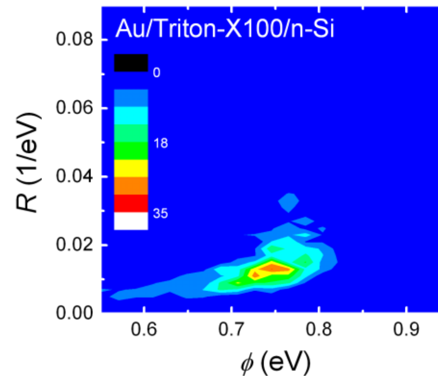

Figure 4: R-ϕ density plot for a Au/Triton-X100/n-Si(111) interface (Sample 3).

Finally, if we add SWNTs to the mix, the interface becomes represented by the R-ϕ density plot in Fig. 5. The addition of SWNT to the Triton-X100 laced Au/*n*-Si interface now appears to further suppress hot electron transmission as evidenced by the general decrease in R. The appearance of two prominent peaks at ~0.75 eV and ~0.80 eV in the distribution likely relates to the emergence of two main types of interface interaction with hot electrons as a result of the presence of Triton-X100 and SWNTs.

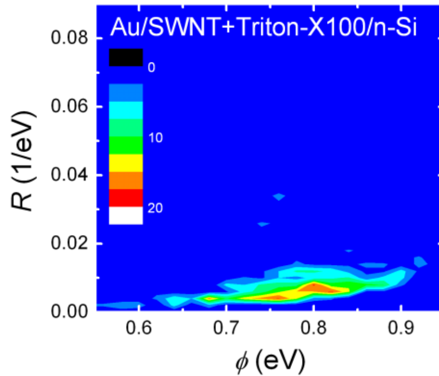

Figure 5: R-ϕ density plot for a Au/SWNT+Triton-X100/n-Si(111) interface.

While a detailed analysis of the density plots in Figs. 4 and 5 is beyond the scope of this paper, it is clear from the above results that the R-ϕ density plot is sensitive to nanoscale changes to the standard Au/n-Si interface. This opens the possibility of using such a dual-parameter representation in conjunction with BEES to provide a way to classify as well as understand interface modifications at the nanoscale level.

5 CONCLUSION

In conclusion, we have presented a study of the Au/n-Si interface modified by organic "contamination" layers intentionally introduced. We show that interface modifications due to an imperfect pentacene film, a film of Triton-X100, and one containing a mixture of SWNTs and Triton-X resulted in significant distinct alterations of the dual-parameter density plot based on the interface transmission attenuation R and barrier height ϕ. This suggests that such a dual-parameter representation may extend the usefulness of BEES data beyond the traditional mapping of BEEM current to a spatial mapping of R and ϕ as we have recently demonstrated [12]. The sensitivity of the R-ϕ density plot to interface modifications may be exploited for interface classification and can potentially enhance our ability to analyze material interface data obtained from nanoscale devices.

ACKNOWLEDGMENTS

We thank Arpun Nagaraja for assistance in preparing the samples modified by Triton-X100 and SWNTs, and performing the BEES measurements.

REFERENCES

[1] International Technology Roadmap for Semiconductors Update 2010, http://public.itrs.net.
[2] W. J. Kaiser and L. D. Bell, Phys. Rev. Lett. 60, 1406, 1988.
[3] L. D. Bell and W. J. Kaiser, Phys. Rev. Lett. 61, 2368, 1988.
[4] M. H. Hecht, L. D. Bell, W. J. Kaiser, and F. J. Grunthaner, Appl. Phys. Lett. 55, 780, 1989.
[5] M. Prietsch and R. Ludeke, Phys. Rev. Lett. 66, 2511, 1991.
[6] H. Sirringhaus, E. Y. Lee, and H. von Känel, Phys. Rev. Lett. 73, 577, 1994.
[7] B. Kaczer and J. P. Pelz, J. Vac. Sci. Technol. B 14, 2864, 1996.
[8] L. Quattropani, I. Maggio-Aprile, P. Niedermann, and Ø. Fischer, Phys. Rev. B 57, 6623, 1998.
[9] H. J. Wen, R. Ludeke, and A. Schenk, J. Vac. Sci. Technol. B 16, 2296, 1998.
[10] Y. Zheng, A. T. S. Wee, Y. C. Ong, K. L. Pey, C. Troadec, S. J. O'Shea, and N. Chandrasekhar, Appl. Phys. Lett. 92, 012914, 2008.
[11] S. Özcan, J. Smoliner, M. Andrews, G. Strasser, T. Dienel, R. Franke, and T.Fritz, Appl. Phys. Lett. 90, 092107, 2007.
[12] K. E. J. Goh, A. Bannani, and C. Troadec, Nanotechnology 19, 445718, 2008.
[13] A. Chahboun, V. Fink, M. Fleischauer, K. L. Kavanagh, R. P. Lu, L. Hansen, C. R. Becker, and L. W. Molenkamp, J. Vac. Sci. Technol. B 20, 1781, 2002.
[14] C. Tivarus, J. P. Pelz, M. K. Hudait, and S. A. Ringel, Phys. Rev. Lett. 94, 206803, 2005.
[15] L. D. Bell and W. J. Kaiser, Annu. Rev. Mater. Sci. 26, 189, 1996.
[16] P. L. de Andres, F. J. Garcia-Vidal, K. Reuter, and F. Flores, Prog. Surf. Sci. 66, 3, 2001
[17] J. Smoliner, D. Rakoczy, and M. Kast, Rep. Prog. Phys. 67, 1863, 2004.
[18] W. Yi, A.J. Stollenwerk, V. Narayanamurti, Surf. Sci. Rep. 64, 169, 2009.
[19] M. Prietsch, Phys. Rep. 253, 163, 1995.
[20] C. Troadec and K. E. J. Goh, J. Vac. Sci. Technol. B 28, C5F1, 2010.
[21] J. C. W. Song, K. E. J. Goh, N. Chandrasekhar, and C. Troadec, Phys. Rev. B 79, 165313, 2009.